

LA-UR-21-25175

Approved for public release; distribution is unlimited.

Title: Overview of FleCSPH Solid Material Modeling Capabilities

Author(s): Sagert, Irina
Korobkin, Oleg
Kaltenborn, Mark Alexander Randolph
Lim, Hyun
Loiseau, Julien
Mauney, Christopher Michael
Tews, Ingo
Tsao, Bing-Jyun
Even, Wesley Paul

Intended for: Report

Issued: 2021-06-01

Disclaimer:

Los Alamos National Laboratory, an affirmative action/equal opportunity employer, is operated by Triad National Security, LLC for the National Nuclear Security Administration of U.S. Department of Energy under contract 89233218CNA000001. By approving this article, the publisher recognizes that the U.S. Government retains nonexclusive, royalty-free license to publish or reproduce the published form of this contribution, or to allow others to do so, for U.S. Government purposes. Los Alamos National Laboratory requests that the publisher identify this article as work performed under the auspices of the U.S. Department of Energy. Los Alamos National Laboratory strongly supports academic freedom and a researcher's right to publish; as an institution, however, the Laboratory does not endorse the viewpoint of a publication or guarantee its technical correctness.

Overview of FleCSPH Solid Material Modeling Capabilities

Irina Sagert, Oleg Korobkin, Alexander Kaltenborn, Hyun Lim, Julien Loiseau, Chris Mauney, Ingo Tews, Bing-Jyun Tsao, Wesley Even

May 10th, 2021

LA-UR-XXXX

Smoothed Particle Hydrodynamics (SPH)

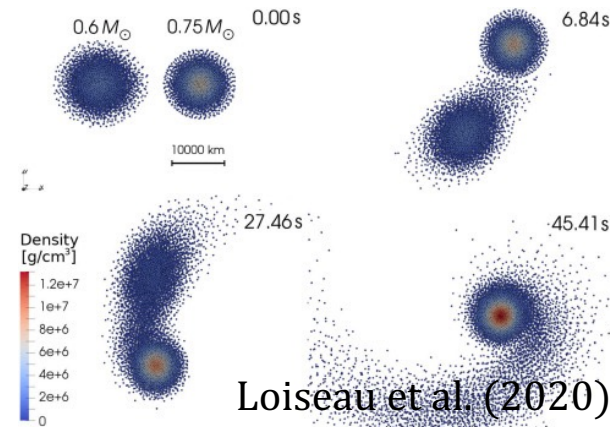
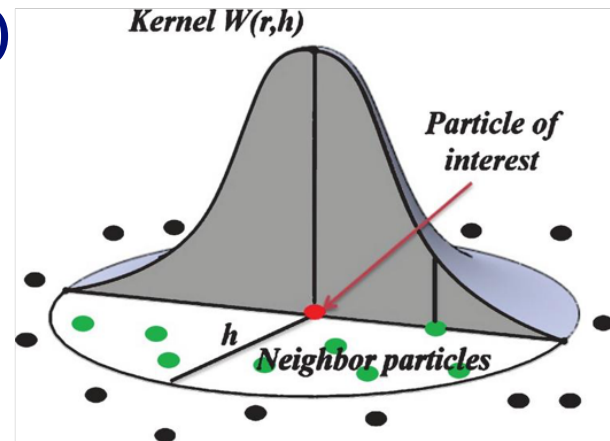
A meshless Lagrangian method where fluid quantities are carried by moving interpolation points (particles with mass) which follow the fluid motion.

A physical quantity at point (or particle) “a” is given by:

$$A(\vec{r})_a = \sum_b \frac{m_b}{\rho_b} A(\vec{r}_b) W(|\vec{r} - \vec{r}_b|, h)$$

SPH Advantages:

- Possesses excellent conservation properties
- Advects quantities exactly (by construction)
- Has resolution where it's needed without remeshing (because the method is mesh-free)
- Angular momentum conservation is built-in, which is difficult to achieve in a grid-based code
- Treatment of vacuum



Loiseau et al. (2020)



FleCSPH

<https://github.com/laristra/flecsph>.



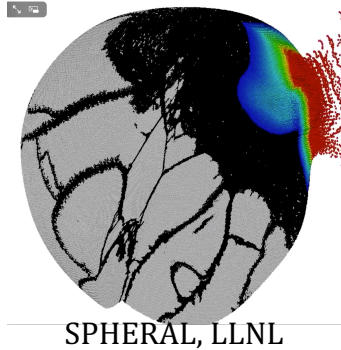
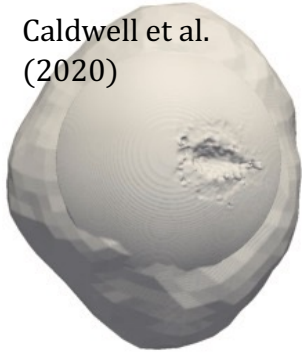
FleCSPH (Loiseau et al., Software X (2020)): SPH code build with the LANL FleCSI numerical framework as part of the LANL Ristra Project. FleCSPH is a **general-purpose SPH code** but has been mainly applied to **astrophysical problems**. Some core capabilities are:

1. Implementation of **different SPH kernels**
2. **Fast-Multipole Method** : A particle-based Poisson solver for Newtonian gravity
3. **Astrophysical EoSs**:
 1. Analytic: Ideal gas, polytropic, piecewise polytropic, cold white dwarf
 2. Tabulated: Finite-temperature nuclear matter (StellarCollapse), Helmholtz
4. **Material EoSs**: Liquid, Mie-Grüneisen, Osborne, Tillotson
5. **External potentials** for boundary conditions and specifying external forces
6. **Fixed general-relativistic background / curvilinear coordinates** for static and rotating stars
7. Strength via the **elastic-perfectly-plastic** (+hardening) model and maximum strain breaking

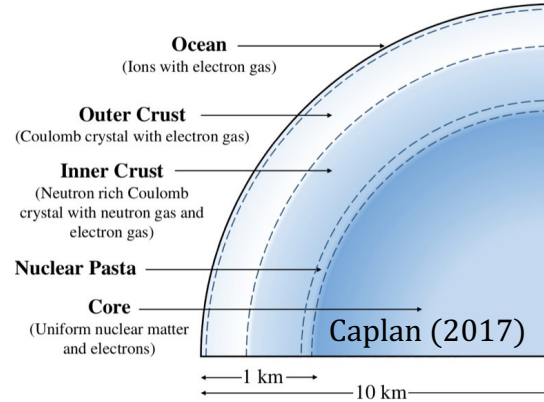


Strength in Astrophysics

Caldwell et al.
(2020)



For **impacts on asteroids**, material strength is a factor in **crater formation**. Including solid material properties into asteroid impact studies improves our understanding of accretion and disruption events in the solar system as well as **planet formation**.



The crust of a neutron star **is the strongest material in Nature**. The crust could play a role in **neutron star mergers**, e.g. break due to tidal forces (Penner et al. (2021), Gittins et al. (2020)) or resonant excitations (Tsang et al. (2021)), or induce a gravitational phase shift via viscous damping (Kochanek (1992)) or elastic-to-plastic transitions (Pan et al. (2020)).

Material Strength Implementation



Conservation Equations

Fluid dynamics codes generally solve the following conservation equations:

1. Conservation of mass: $\frac{d\rho}{dt} = -\rho \frac{\partial v^\alpha}{\partial x^\alpha}$
2. Conservation of momentum: $\frac{dv^\alpha}{dt} = \frac{1}{\rho} \frac{\partial \sigma^{\alpha\beta}}{\partial x^\beta}$
3. Conservation of energy: $\frac{du}{dt} = -\frac{\sigma^{\alpha\beta}}{\rho} \frac{\partial v^\alpha}{\partial x^\beta}$

The form of the stress tensor $\sigma^{\alpha\beta}$ depends on the modeled material, e.g.

$$\begin{aligned}\sigma^{\alpha\beta} &= P\delta^{\alpha\beta} \text{ (gas)} \\ \sigma^{\alpha\beta} &= P\delta^{\alpha\beta} + S^{\alpha\beta} \text{ (solid)}\end{aligned}$$



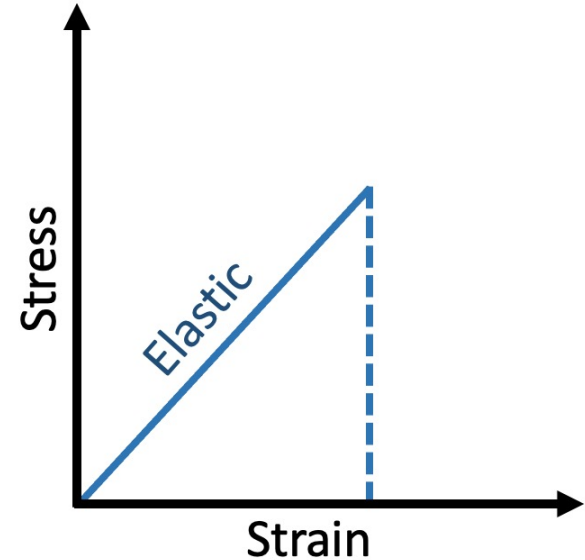
Elasticity

While information on the pressure is obtained from a given **equation of state**, the information on the deviatoric stress tensor $S^{\alpha\beta}$ given a specific deformation, is provided by an **elasticity/plasticity** model.

For elasticity, the simplest example is **Hooke's Law** where $S^{\alpha\beta}$ is given in terms of the strain tensor $\epsilon^{\alpha\beta}$:

$$S^{\alpha\beta} = 2\mu \left(\epsilon^{\alpha\beta} - \frac{1}{3} \epsilon^{\gamma\gamma} \delta^{\alpha\beta} \right)$$

with a material-dependent shear modulus μ .



Plasticity

For large strains, material can undergo plastic deformation.

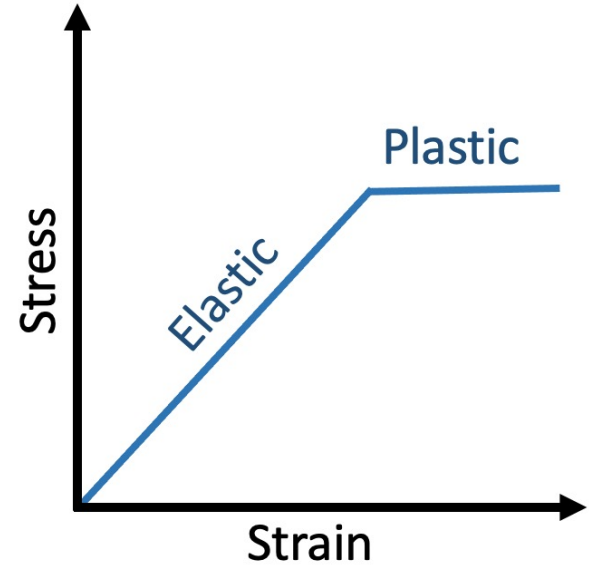
We need to know a **yield criterion** (i.e. when plasticity sets in) and have a corresponding model for the behavior of $S^{\alpha\beta}$. One successful criterion is the **van-Mises yielding criterion**:

$$\sigma_v = \sqrt{3J_2} = \sqrt{\frac{3}{2} S^{\alpha\beta} S^{\alpha\beta}}$$

which is used in the **perfectly plastic model** to limit :

$$S^{\alpha\beta} \rightarrow fS^{\alpha\beta} = \min \left[\frac{Y_0}{\sigma_v}, 1 \right] S^{\alpha\beta}$$

i.e. yielding sets in when the 2nd deviator stress invariant J_2 reaches or exceeds the yield strength Y_0 .



Conservation Equations for the Elastic-Perfectly-Plastic Model

1. Conservation of mass: $\frac{d\rho}{dt} = -\rho \frac{\partial}{\partial x^\alpha} v^\alpha$

2. Conservation of momentum:

$$\frac{dv^\alpha}{dt} = \frac{1}{\rho} \frac{\partial}{\partial x^\beta} (-P\delta^{\alpha\beta} + fS^{\alpha\beta}), \quad f = \min \left[\frac{Y_0}{\sigma_v}, 1 \right], \quad \sigma_v = \sqrt{\frac{3}{2} S^{\alpha\beta} S^{\alpha\beta}}$$

3. Conservation of energy: $\frac{du}{dt} = -\frac{P}{\rho} \frac{\partial}{\partial x^\alpha} v^\alpha + \frac{1}{\rho} f S^{\alpha\beta} \dot{\epsilon}^{\alpha\beta}$

4. Time evolution of the deviatoric stress tensor:

$$\frac{dS^{\alpha\beta}}{dt} = 2\mu \left(\dot{\epsilon}^{\alpha\beta} - \frac{1}{3} \dot{\epsilon}^{\gamma\gamma} \delta^{\alpha\beta} \right) + f S^{\alpha\gamma} \dot{R}^{\gamma\beta} - \dot{R}^{\alpha\gamma} f S^{\gamma\beta}$$



SPH Discretization of the Elastic-Perfectly-Plastic Model:

1. $\frac{d\rho_a}{dt} = -\rho_a \sum \frac{m_b}{\rho_b} v_{ab}^\alpha \frac{\partial W_{ab}}{\partial x_a^\alpha}$
 2. $\frac{dv_a^\alpha}{dt} = -\sum m_b \left[\left(\frac{P_a}{\rho_a^2} + \frac{P_b}{\rho_b^2} + \Pi_{ab} \right) \frac{\partial W_{ab}}{\partial x_a^\alpha} - \left(\frac{S_a^{\alpha\beta}}{\rho_a^2} + \frac{S_b^{\alpha\beta}}{\rho_b^2} \right) \frac{\partial W_{ab}}{\partial x_a^\beta} \right]$
 3. $\frac{du_a}{dt} = \sum m_b \left(\frac{P_a}{\rho_a^2} + \frac{\Pi_{ab}}{2} \right) v_{ab}^\alpha \frac{\partial W_{ab}}{\partial x_a^\alpha} + \frac{S_a^{\alpha\beta}}{\rho_a} \dot{\epsilon}^{\alpha\beta}$
 4. $\frac{dS^{\alpha\beta}}{dt} = 2\mu \left(\dot{\epsilon}^{\alpha\beta} - \frac{1}{3} \dot{\epsilon}^{\gamma\gamma} \right) + S^{\alpha\gamma} \dot{R}^{\gamma\beta} - \dot{R}^{\alpha\gamma} S^{\gamma\beta}$
- Strain rate tensor: $\dot{\epsilon}^{\alpha\beta} = \frac{1}{2\rho_a} \sum m_b \left[v_{ba}^\alpha \frac{\partial W_{ab}}{\partial x_a^\beta} + v_{ba}^\beta \frac{\partial W_{ab}}{\partial x_a^\alpha} \right]$
 - Rotation rate tensor: $\dot{R}^{\alpha\beta} = \frac{1}{2\rho_a} \sum m_b \left[v_{ba}^\alpha \frac{\partial W_{ab}}{\partial x_a^\beta} - v_{ba}^\beta \frac{\partial W_{ab}}{\partial x_a^\alpha} \right]$



Maximum-Strain Damage Model

To simulate material failure, damage is often treated as a state variable and evolved in time to describe the growth of cracks.

We are currently using a **maximum-strain damage model** in which failure occurs once the breaking strain is reached.

In order to determine if a particle exceeds the breaking strain during the simulation, we derive the local scalar strain from the 3D stress.

For this, we compute the local scalar strain from the maximum tensile stress $\sigma_{\max} = \max[\sigma_1, \sigma_2, \sigma_3]$ where σ_γ are the principal stresses determined by a principal axis transformation of the stress tensor $\sigma^{\alpha\beta}$.

The local strain is given by $\epsilon = \frac{\sigma_{\max}}{E}$, $E = \frac{9K\mu}{3K+\mu}$.



Plasticity – Linear Isotropic Hardening

We calculate the **increment of plastic strain**:

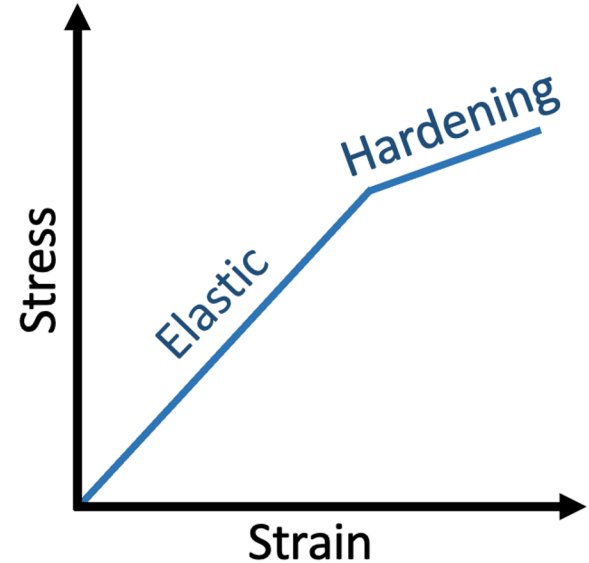
$$\Delta\epsilon_p = \frac{\sigma_v - Y(\epsilon_p)}{3\mu + H}$$

The yield stress is incremented according to:

$$Y(\epsilon_p + \Delta\epsilon_p) = Y_0 + H(\epsilon_p + \Delta\epsilon_p),$$

with the **hardening modulus** H . The deviatoric stress is update according to

$$S^{\alpha\beta} \rightarrow fS^{\alpha\beta} = \min\left[\frac{Y}{\sigma_v}, 1\right] S^{\alpha\beta}$$



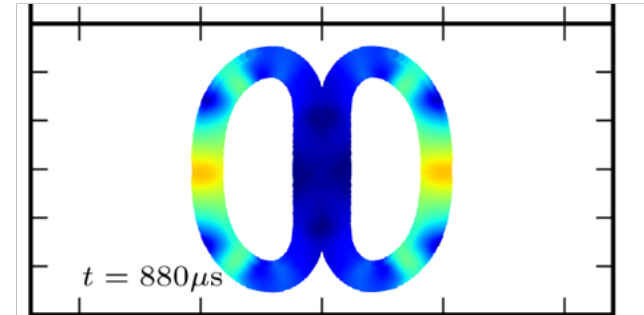
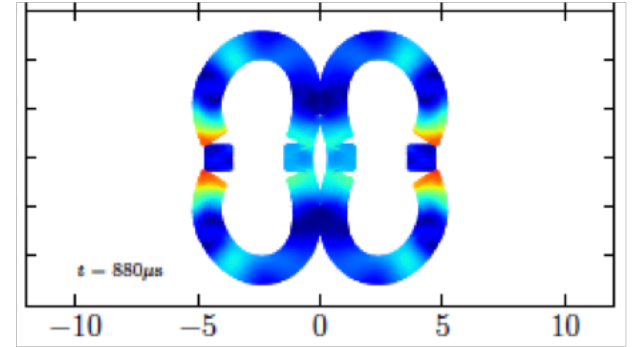
Tensile Instability:

The so-called **tensile instability** can occur in SPH when negative pressure or tension is present. The instability leads to artificial **numerical clumping** of particles which then results in **unphysical fragmentation**.

One way to overcome the tensile instability is to add a small repulsive artificial stress $\xi^{\alpha\beta}$:

$$\frac{dv_a^\alpha}{dt} = - \sum m_b \left[\left(\frac{\sigma_a^{\alpha\beta}}{\rho_a^2} + \frac{\sigma_b^{\alpha\beta}}{\rho_b^2} + \xi_{ab}^{\alpha\beta} \left(\frac{W_{ab}}{W_{dx}} \right)^n + \Pi_{ab} \right) \frac{\partial W_{ab}}{\partial x_a^\alpha} \right]$$

where $\xi_a^{\alpha\beta} = -\epsilon_s \frac{\sigma_a^{\alpha\beta}}{\rho_a^2}$ and is set to 0 for compression.



Schaefer et al. A&A 590 (2016)



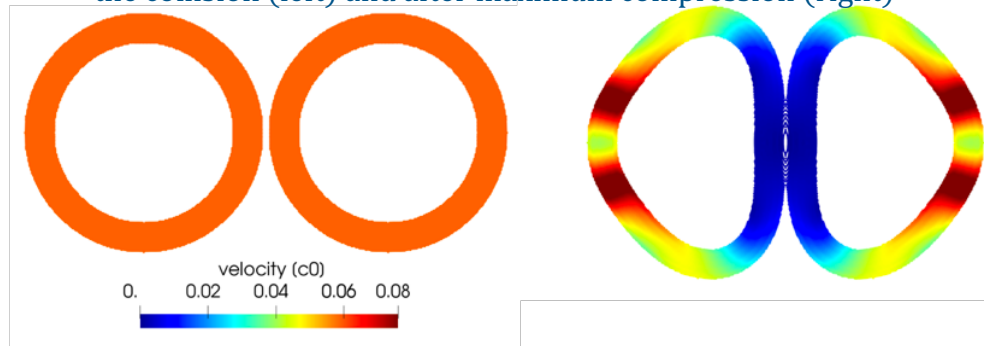
Numerical Tests



Colliding Rubber Rings

A test for the **numerical implementation of elasticity** (Swegle 1992, Gray et al. 2001, Schäfer 2005).

Fig.: Colliding rubber rings modeled with FleCSPH before the collision (left) and after maximum compression (right)

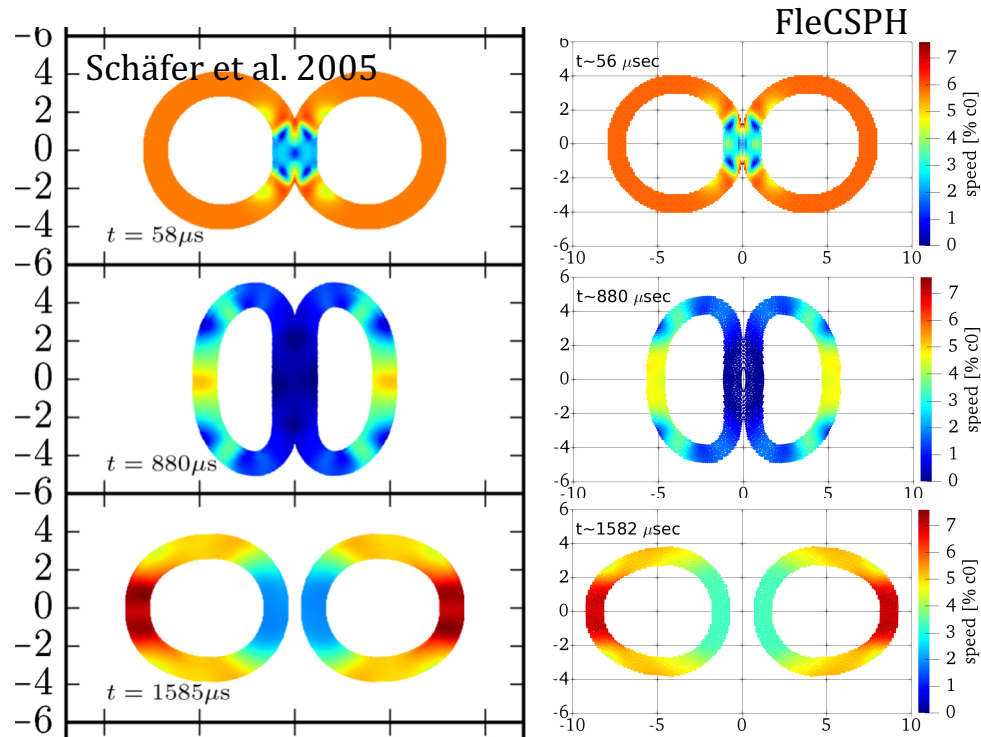


- Two rubber rings with a density of $\rho_0 = 1.01 \text{ g/cm}^3$, sound speed $c_0 = 8.54 \times 10^4 \text{ cm/s}$, shear modulus $\mu = 0.22 \rho_0 c_0^2$ collide at $0.118 c_0$.
- The rings have an initial inner and outer radius of 3cm and 4cm, respectively.
- The pressure is given by the liquid EoS
- The basic test includes elasticity only but we also test the effect of plasticity and breaking

After colliding, the rings bounce off each other, and begin to swing as they move in opposite directions. While simple, the setup is powerful in testing **artificial fragmentation** due to tensile instability, **symmetry** of the code, and **dissipation**.

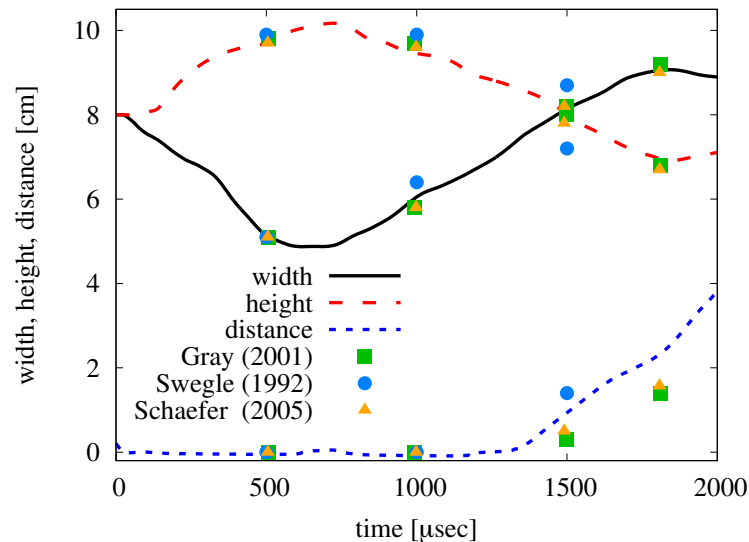


Colliding Rubber Rings



Figs.: Colliding rubber rings modeled with an SPH code by Schaefer et al. (left) and results of a similar setup with FleCSPH (middle).

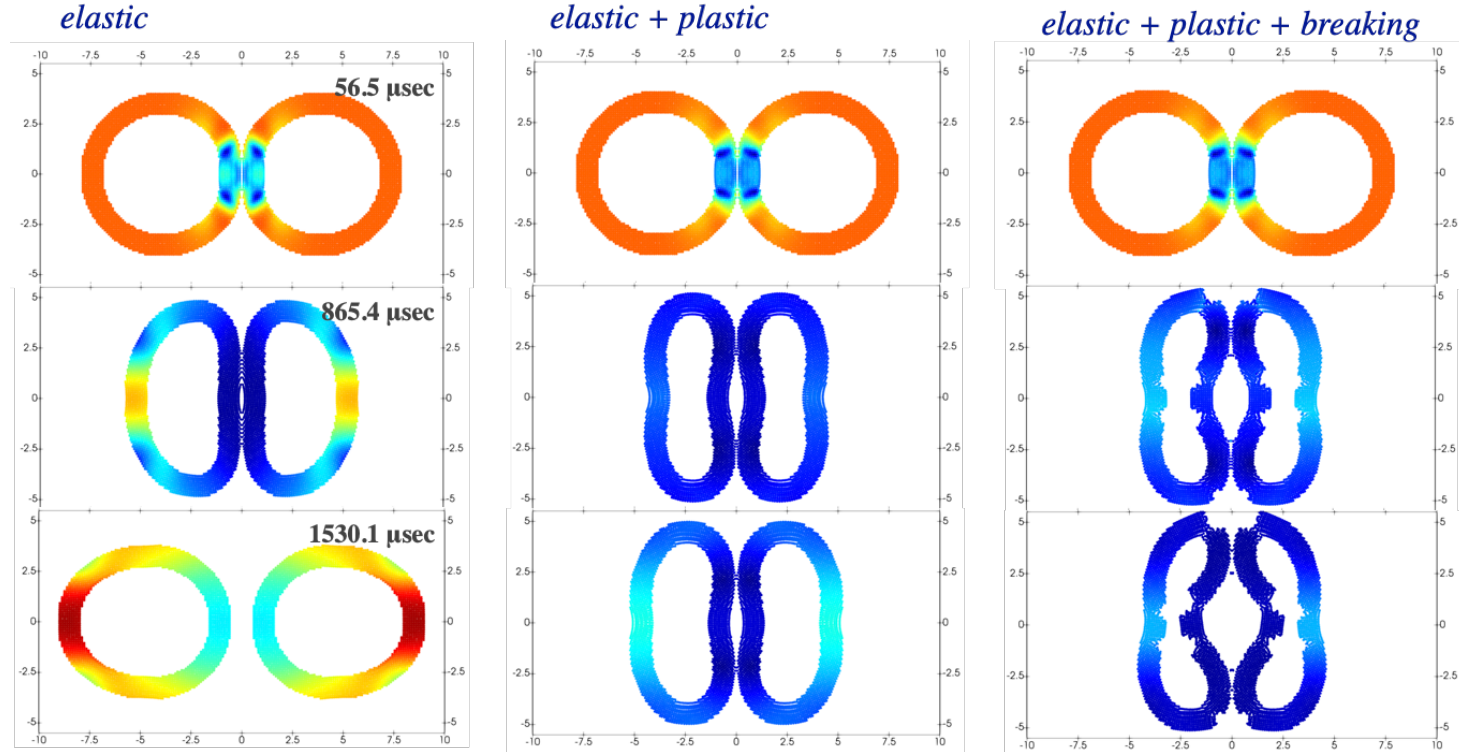
Bottom: Comparison of ring width, height, and distance between different SPH and Eulerian codes (points) including FleCSPH (lines).



We find good agreement of the velocity distribution and the ring geometry with previous studies.



Colliding Rubber Rings



Some preliminary tests with plasticity and breaking have been performed

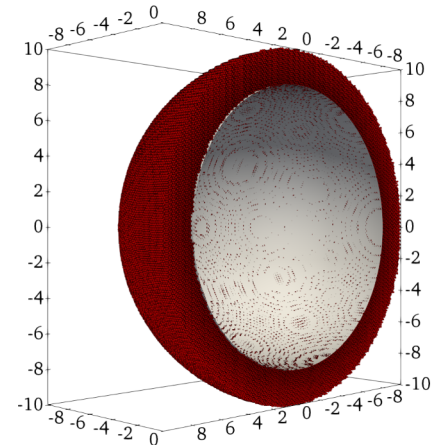
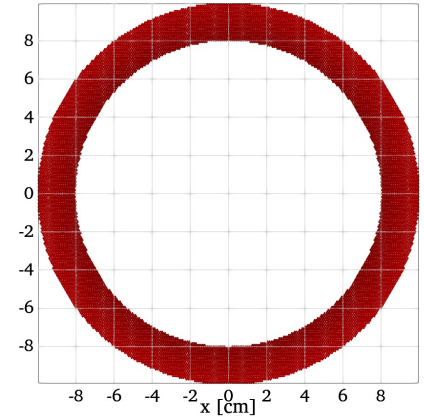


Verney Implosion

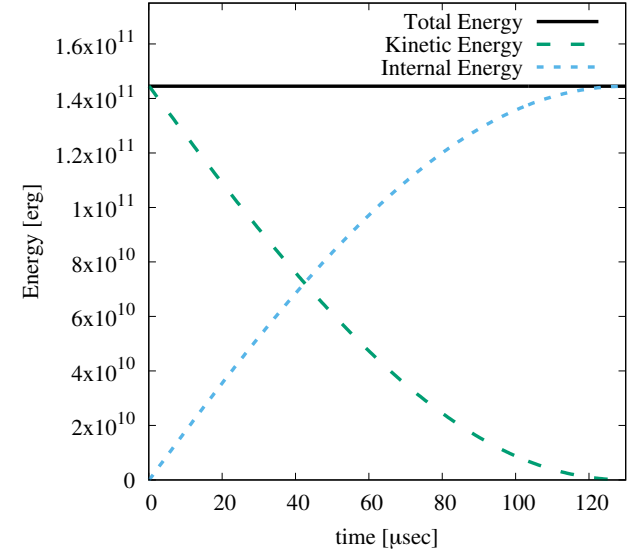
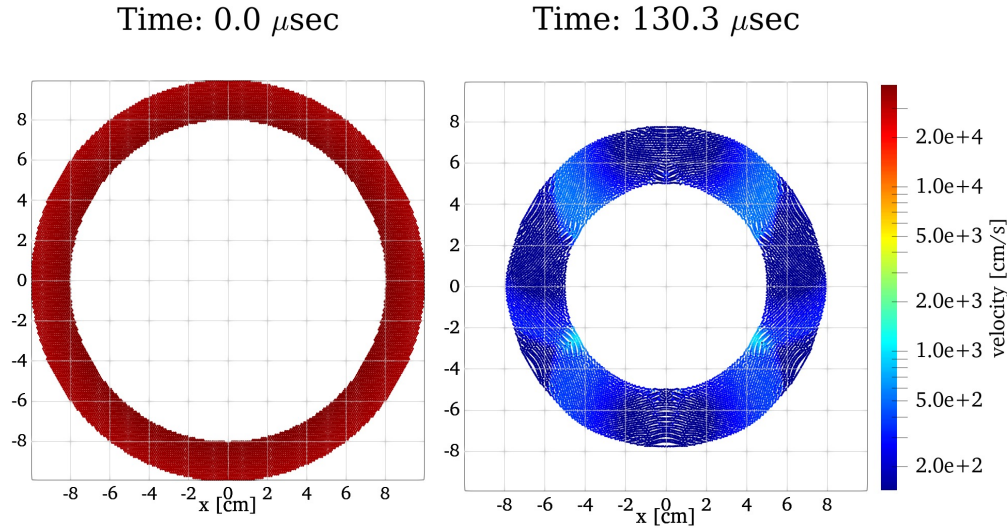
(e.g. Howell & Ball, JCP 175 (2002))

- A metal shell receives a radial inward velocity
- During the convergence, the shell thickens and its **kinetic energy is converted into internal energy** through the **dissipative plastic distortion** mechanism.
- The collapse terminates at a stopping radius which is a function of the initial conditions.
- The test is done in 2D (cylindrical shell) and 3D (spherical shell).
- The metal shell is made of Beryllium and described by the Osborne material EoS.
- The strength model is elastic-perfectly-plastic with $\mu = 1.5111 \times 10^{11}$ Ba and $Y_0 = 3.3 \times 10^9$ Ba

Time: 0.0 μsec



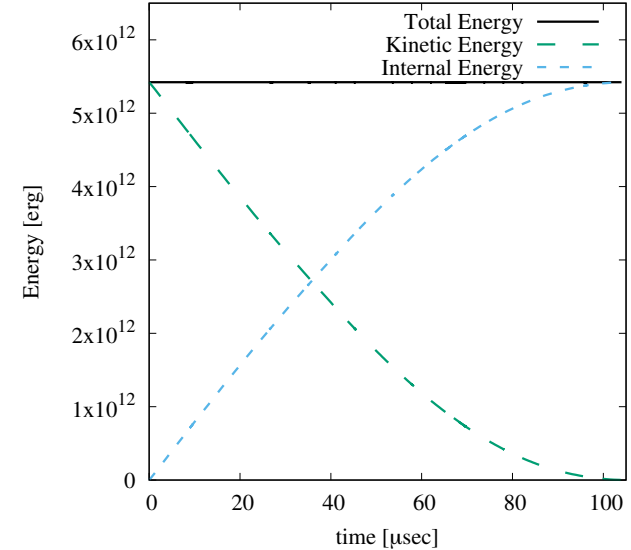
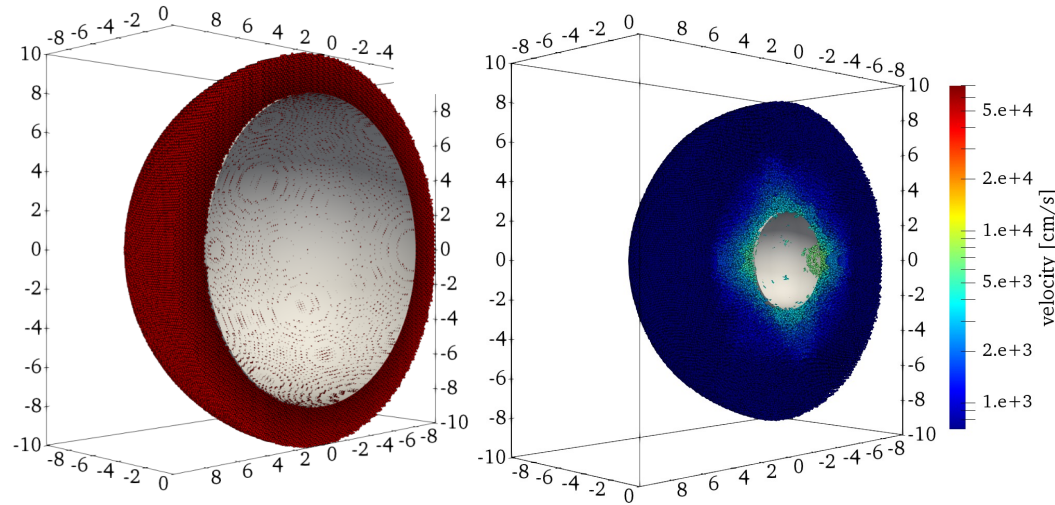
2D Verney Implosion



- Initial radial velocity is set to $v_r(r) = (R_{inner}/r) v_0$ with $v_0 = 41710$ cm/s and R_{inner} being the initial inner radius of 8cm.
- For a final inner radius of 5cm the stopping time is about 127 μsec . We recover this time when ca. 99.9% of the initial kinetic energy is dissipated into internal energy.
- The radial distance of inner particles at stopping time is 5cm with a variation of max. 2%.



3D Verney Implosion



- Initial radial velocity is set to $v_r(r) = (R_{inner}/r)^2 v_0$ with $v_0 = 67750 \frac{\text{cm}}{\text{s}}$
- For a final inner radius of 3cm the stopping time is about 100μsec. We recover this time when ca. 99.9% of the initial kinetic energy is dissipated into internal energy.
- The radial distance of inner particles at stopping time is ca. 3cm with about 1.4% of particles having a smaller radial distance with $2.5\text{cm} < r < 3.0\text{cm}$



Taylor Anvil

(e.g. Burton et al., JPC 2015)

- A **cylindrical copper rod** with radius 0.32cm and length 3.24cm impacts a rigid surface at a velocity of 227 m/s.
- There are no analytical results for this particular test problem but we can compare to e.g. other codes.
- **Material properties:** $\rho_0 = 8.930$ g/cc, shear modulus $\mu = 4.3333 \times 10^{11}$ Ba, yield stress $Y_0 = 4 \times 10^9$ Ba, hardening modulus $Y_H = 10^9$ Ba, and Grüneisen EoS with $c_0 = 3.94 \times 10^5$ cm/s, $s = 1.48$, $\Gamma = 2.0$.
- At 80 μ sec we find a height ~ 2.17 cm and foot radius ~ 0.66 cm which is in good comparison to published results

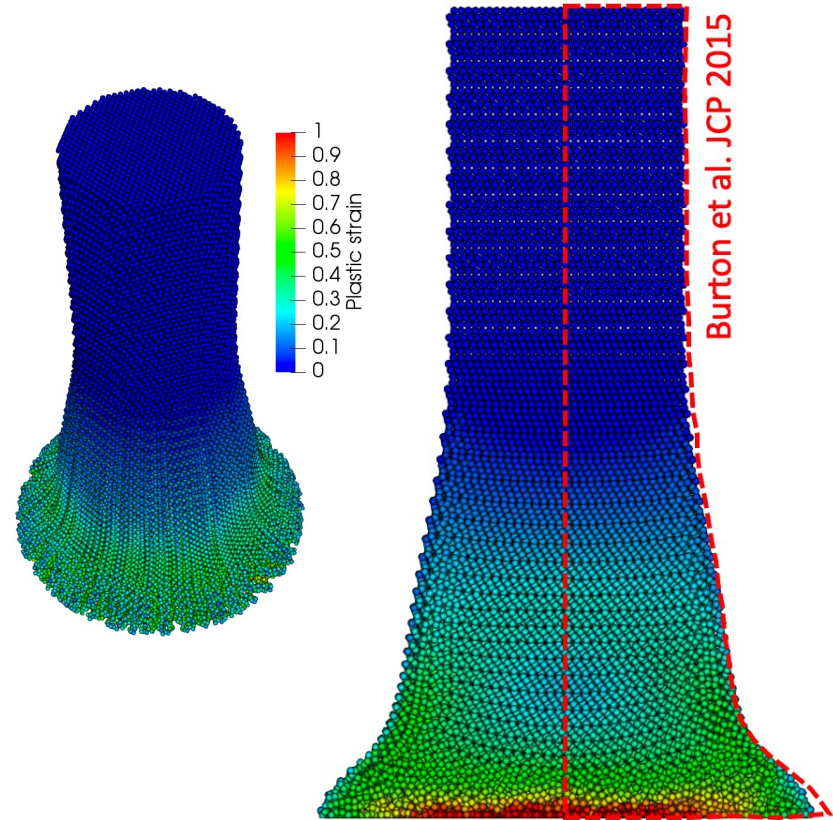
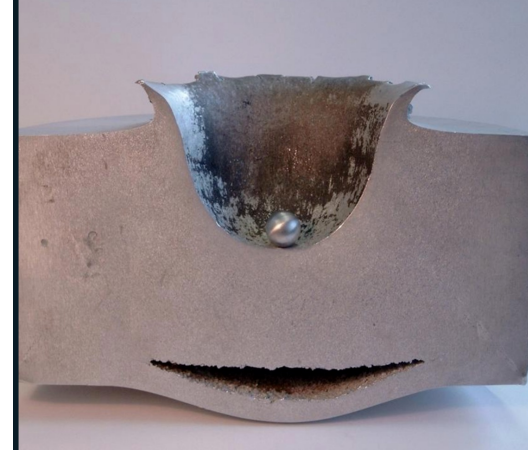
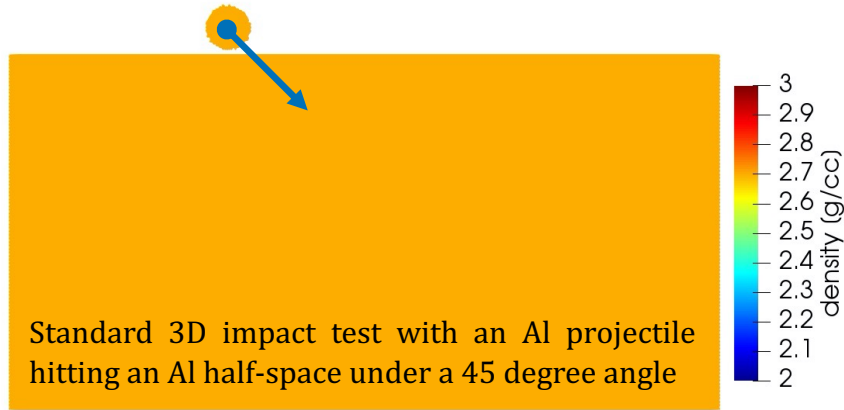


Fig.: Taylor anvil shape at 80 μ sec from FleCSPH together with the outline (red dashed line) of the anvil from Burton et al. at the same time.

Impact Simulations



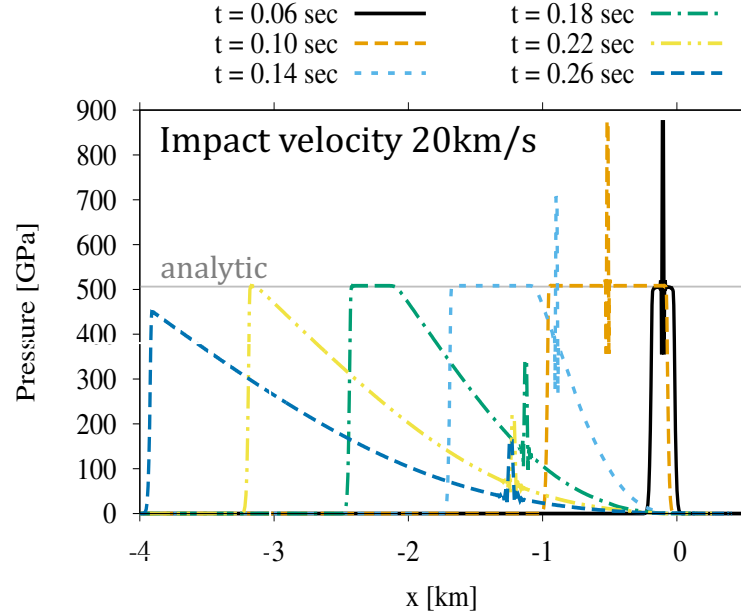
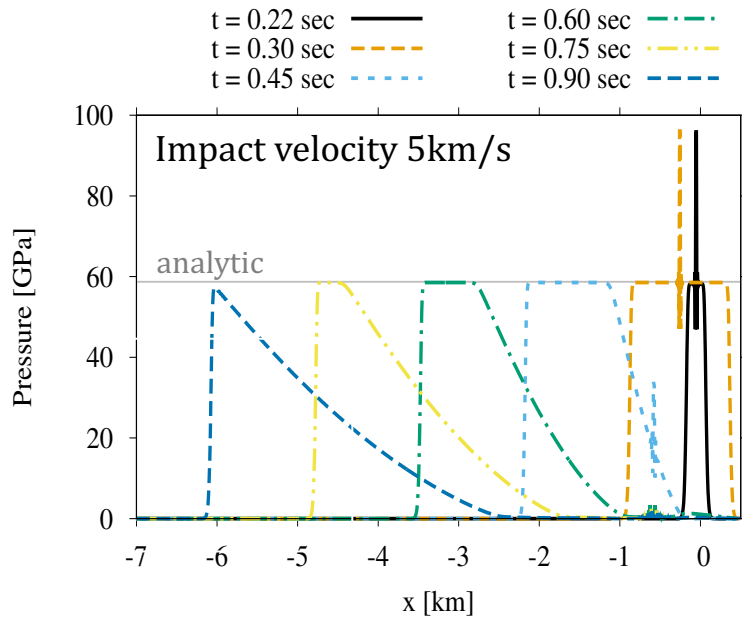
ESA: Lab test impact between a small sphere of Al traveling at ca. 6.8km/s and a block of Al 18cm thick. This test simulates what can happen when a small space debris object hits a spacecraft.

Simplified impact simulations can verify a code's capability to model the initial stages of crater formation - contact, compression and begin of the excavation process for a given material EoS.

Since strength does not play a significant role for the dynamical evolution, it is not included in this setup. The target and projectile are composed of Aluminum and modeled with the Al-6061 Mie-Grüneisen EoS.



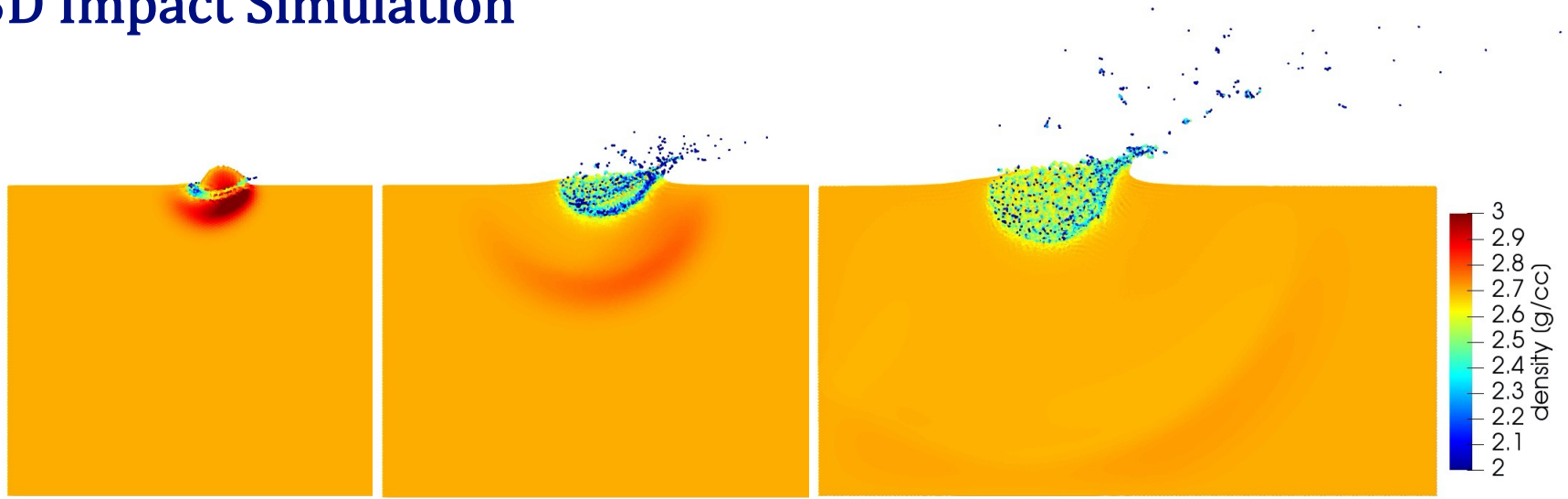
1D Impact Simulation



For 1D simulations, we can compare the maximum pressure at the impact site to an analytic solution $P = \rho_0 (c_0 + s v_p) v_p$ where v_p is the particle velocity. The initial density of projectile and target is set to $\rho_0 = 2.7 \frac{\text{g}}{\text{cm}^3}$ while the sound speed $c_0 = 5.35 \cdot 10^5 \frac{\text{cm}}{\text{s}}$



3D Impact Simulation



3D impact simulations do not have an analytic solution. However, we can still compare the maximum pressure close to the impact site and its decrease with distance and time. Furthermore, in a 45 degree impact, it is expected that the projectile fragments with parts of it being ejected out of the impact site which we can also see in our simulations.

Summary & Outlook

- Solid material modeling has been implemented into the LANL SPH code FleCSPH
- FleCSPH now contains the **elastic – perfectly plastic material model**, **plastic hardening**, and **maximum-strain breaking**
- Elasticity and plasticity have been tested via the **Colliding Rubber Ring** test, the **Verney Implosion**, and the **Taylor Anvil** test
- FleCSPH also contains several analytic material equations of state: **Mie-Grueneisen**, **Osborne**, and the **Tillotson**
- 1D-3D Impact simulations have been used for testing the material EoS implementations
- The planned astrophysical application for FleCSPH to study neutron star crust dynamics only requires the elastic - perfectly plastic material modeling with maximum strain breaking. However, it would be interesting to implement and test more advanced strength and damage models. Other possible future goals are the implementation of **tabulated material EoSs**, like Sesame tables, and **multi-material modeling**.



Backup Slides



Equations of State in FleCSPH

Astrophysical EoSs:

- **Analytical:** Ideal fluid, Polytropic and Piecewise Polytropic, Cold White Dwarf Matter
- **Tabulated:** Nuclear for Astrophysics (StellarCollapse EoSs), Helmholtz

Solid Material EoSs:

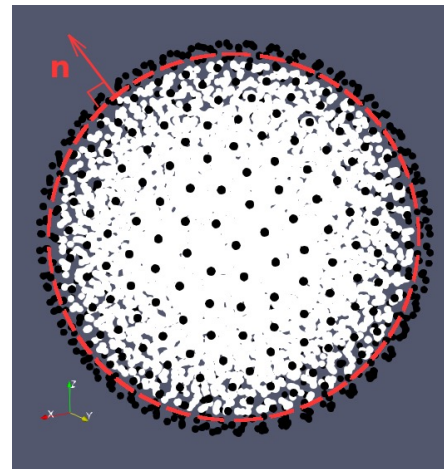
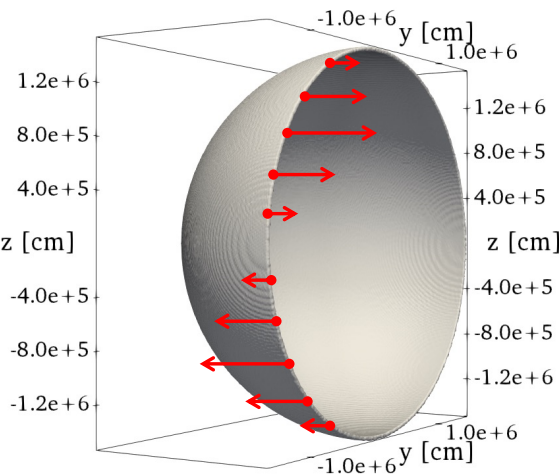
- Liquid: $P(\rho) = c_0^2 (\rho - \rho_0)$
- Mie-Grüneisen (also in the Wilkins form): $P(\rho, u) = \rho_0 c_0^2 \chi \left[1 - \frac{\Gamma_0}{2} \chi \right] (1 - s\chi)^{-2} + \Gamma_0 \rho u$, $\chi = 1 - \frac{\rho_0}{\rho}$
- Osborne: $P(\rho, u) = \frac{a_1 \eta + \bar{a} \eta^2 + E'(b_0 + b_1 \eta + b_2 \eta^2) + E'^2(c_0 + c_1 \eta)}{E' + e_0}$, $\eta = \frac{\rho}{\rho_0} - 1$, $E' = u \rho_0$
- Tillotson: $P(\rho, u) = \begin{cases} \Gamma_I E \rho + A \mu + B \mu^2, \eta = \frac{\rho}{\rho_0}, \mu = \eta - 1; \text{ for } \rho \geq \rho_0 \text{ or } \rho < \rho_0, E < E_s \\ a E \rho + \left(b E \rho \left(\frac{E}{E_0 \eta^2} + 1 \right)^{-1} + A \exp[-\alpha(\eta^{-1} - 1)] \right) \exp[-\beta(\eta^{-1} - 1)^2]; \text{ for } \rho < \rho_0, E \geq E'_s \\ [P_{IV}(E - E_s) + P_{II}(E'_s - E)] (E'_s - E_s); \text{ for } \rho < \rho_0, E_s \leq E < E'_s \end{cases}$



Boundary Conditions

- FleCSPH has simple boundary conditions such as **periodic**, **frozen**, and **reflective**
- In addition, the code can use **external potentials and potential walls**
- **Solid-fluid boundary interactions** are currently being implemented. These are important for e.g. modeling the dynamics of neutron stars with a fluid core and solid crust where the shear motions of crust and core must be completely decoupled from each other.

A cut of a thin shell of the neutron star crust with imposed toroidal velocity (red arrows). The shell is dynamically evolved and kept stable via external potentials and potential walls



Neutron star in FleCSPH with a fluid core (white) and solid crust (black). The red line shows the core-crust transition. Specific boundary conditions must be implemented at the interface to decouple their shear motion of crust and core.

